Universiteit Antwerpen

This item is the archived peer-reviewed author-version of:

Chromium speciation methods and infrared spectroscopy for studying the chemical reactivity of lead chromate-based pigments in oil medium

Reference:

Monico Letizia, Janssens Koen, Cotte Marine, Sorace Lorenzo, Vanmeert Frederik, Brunetti Brunetto Giovanni, Miliani Costanza.- Chromium speciation methods and infrared spectroscopy for studying the chemical reactivity of lead chromate-based pigments in oil medium

Microchemical journal - ISSN 0026-265X - Amsterdam, Elsevier science bv, 124(2016), p. 272-282

Full text (Publishers DOI): http://dx.doi.org/doi:10.1016/j.microc.2015.08.028

To cite this reference: http://hdl.handle.net/10067/1310990151162165141

uantwerpen.be

Institutional repository IRUA

Accepted Manuscript

Chromium speciation methods and infrared spectroscopy for studying the chemical reactivity of lead chromate-based pigments in the oil medium

Letizia Monico, Koen Janssens, Marine Cotte, Lorenzo Sorace, Frederik Vanmeert, Brunetto Giovanni Brunetti, Costanza Miliani

PII: S0026-265X(15)00202-7
DOI: doi: 10.1016/j.microc.2015.08.028
Reference: MICROC 2231

To appear in: *Microchemical Journal*

Received date: 29 July 2015
Accepted date: 23 August 2015

Please cite this article as: Letizia Monico, Koen Janssens, Marine Cotte, Lorenzo Sorace, Frederik Vanmeert, Brunetto Giovanni Brunetti, Costanza Miliani, Chromium speciation methods and infrared spectroscopy for studying the chemical reactivity of lead chromate-based pigments in the oil medium, *Microchemical Journal* (2015), doi: 10.1016/j.microc.2015.08.028

This is a PDF file of an unedited manuscript that has been accepted for publication. As a service to our customers we are providing this early version of the manuscript. The manuscript will undergo copyediting, typesetting, and review of the resulting proof before it is published in its final form. Please note that during the production process errors may be discovered which could affect the content, and all legal disclaimers that apply to the journal pertain.

ACCEPTED MANUSCRIPT

Chromium speciation methods and infrared spectroscopy for studying the chemical reactivity of lead chromate-based pigments in the oil medium

Letizia Monico,[1,2,*] *Koen Janssens,*[2] *Marine Cotte,*[3,4] *Lorenzo Sorace,*[5] *Frederik Vanmeert,*[2] *Brunetto Giovanni Brunetti,*[1] *Costanza Miliani*[1]

[1] CNR-Institute of Molecular Science and Technologies (ISTM) and Centre SMAArt, c/o Department of Chemistry, Biology and Biotechnologies, University of Perugia, via Elce di Sotto 8, 06123 Perugia, Italy.

[2] Department of Chemistry, University of Antwerp, Groenenborgerlaan 171, 2020 Antwerp, Belgium.

[3] European Synchrotron Radiation Facility (ESRF), Avenue des Martyrs 71, 38000 Grenoble, France.

[4] Laboratoire d'Archéologie Moléculaire et Structurale (LAMS), CNRS-UPMC, UMR 8220, place Jussieu 4, 75005 Paris, France.

[5] Department of Chemistry "U. Schiff" and INSTM RU, University of Florence, Via della Lastruccia 3-13, 50019 Sesto Fiorentino, Italy.

[*] Correspondence: letizia.monico@uantwerpen.be

ACCEPTED MANUSCRIPT

ACCEPTED MANUSCRIPT

ABSTRACT

Environmental factors, such as light, humidity and temperature are triggering agents for the alteration of organic and/or inorganic constituents of oil paintings. The oxidation of the organic material is favored by increasing of relative humidity and temperature, whereas processes involving changes of the oxidation states of a number of inorganic pigments (*e.g.*, vermilion, cadmium yellows, zinc yellows, chrome yellows) are mainly activated by light-exposure.

In view of the optimization of the long-term conservation and restoration strategies of paintings it is of relevant interest to establish the consequences of thermal parameters (temperature and relative humidity) on the chemical/photochemical-reactivity and the nature of the alteration products of light sensitive-pigments in the oil medium.

To this aim here we propose a multi-method analytical approach based on the combination of diffuse reflectance UV-Vis, FTIR, synchrotron radiation (SR)-based micro X-ray fluorescence (μ-XRF)/micro-X-ray absorption near edge structure (XANES) and electron paramagnetic resonance (EPR) spectroscopies for studying the effects of different relative humidity conditions before and after light exposure on the reactivity of a series of lead chromate-based pigments [such as $PbCrO_4 \cdot PbO$ (monoclinic), $PbCrO_4$ (monoclinic) and $PbCr_{0.2}S_{0.8}O_4$ (orthorhombic)] in an oil medium. The investigation of paint models was also compared to that of a late 19^{th} century historical orthorhombic $PbCr_{0.4}S_{0.6}O_4$ oil paint.

Diffuse reflectance UV-Vis and FTIR spectroscopies were used to obtain information associated with chromatic changes and the formation of organo-metal degradation products at the paint surface. SR-based Cr K-edge μ-XANES/μ-XRF mapping analysis and EPR spectroscopy were employed in a complementary fashion to determine the amount, nature and distribution of Cr(III) and Cr(V)-based alteration compounds within the paints with micrometric spatial resolution.

Under the employed thermal aging conditions, lead(II)-carboxylates and reduced Cr-compounds (in abundance of up to about 35% at the surface) have been identified in the lead chromate-based paints. The tendency of chromates to become reduced increased with increasing moisture levels and

ACCEPTED MANUSCRIPT

was favored for the orthorhombic $PbCr_{0.2}S_{0.8}O_4$ compounds. The redox process gave rise to the formation of Cr(V)-species in relative amount much higher than that was formed in the equivalent paint which was exposed only to light.

After light-exposure of the thermally aged paints, compounds ascribable to the oxidation of the organic binder were detected for all the types of pigments. Nevertheless, the previous thermal treatment increased the tendency towards photo-reduction of only the $PbCr_{0.2}S_{0.8}O_4$ pigment. For this light-sensitive compound, the thickness variation of the reduced Cr-rich (*ca.* 70%) photo-alteration layer with moisture levels could be ascribed to a surface passivation phenomenon that had already occurred before photochemical aging.

KEYWORDS: chrome yellows, Van Gogh, lead carboxylates, reduction, electron paramagnetic resonance, synchrotron.

ACCEPTED MANUSCRIPT

ACCEPTED MANUSCRIPT

1. INTRODUCTION

Oil paintings are complex and heterogeneous systems whose appearance and structural integrity over time is influenced by chemical transformations of their organic/inorganic constituents. These reactions might be activated or accelerated by environmental factors, such as light, moisture, heat, atmospheric pollutants, storage conditions or specific conservation and restoration interventions [1]. Studies on both micro-samples taken from 16^{th}-20^{th} century paintings and on aged model samples have extensively documented that carboxylates of metal ions (soaps) [2,3,4,5] and secondary products (*e.g.,* amorphous, inorganic/organo-metal compounds) arising from changes of the oxidation state of the metal of the pigment [6,7] are common alteration products of oil paintings.

Free fatty acids result from the hydrolysis of triglycerides in the drying oil binder and reacting with metal compounds (that can be present as pigments, fillers, or driers), may form metal carboxylates: soaps of Pb(II) [8,9,10,11], Zn(II) [2,12,13], K^+ [14], Ca(II) and Cu(II) [15,16,17] have been frequently encountered in oil paintings. Humidity and temperature [18,19] as well as paint additives [20] play a key role in the process of formation of metal soaps. They may be present in the form of large aggregates, as superficial deposits or homogeneously distributed throughout the paint layers.

Metal soaps have been characterized by various techniques, such as X-ray diffraction (XRD) [21,22], nuclear magnetic resonance (NMR) spectroscopy [23,24] and a range of vibrational spectroscopic and mass spectrometry techniques [3-5,12-19].

The redox reactions that cause the formation of secondary compounds of various pigments, including vermilion red (HgS) [25,26], realgar/orpiment (arsenic sulfide-based compounds) [27], cadmium yellow (cadmium sulfide-based materials) [28,29,30,31], Prussian blue ($MFe^{III}[Fe^{II}(CN)_6]\cdot xH_2O$, with $M=K^+$, NH_4^+ or Na^+) [32,33], zinc yellow ($K_2O\cdot 4ZnCrO_4\cdot 3H_2O$) [34], and red lead ($Pb_3O_4$) [35], are primarily activated by light (sometimes in combination with humidity and/or environmental pollutants). In these cases, the degradation products are formed as a layer of limited thickness (below 100 µm) at the paint surface.

ACCEPTED MANUSCRIPT

Synchrotron radiation (SR)-based X-ray microprobe techniques, such as micro X-ray fluorescence (μ-XRF), micro-X-ray absorption near edge structure (XANES) and μ-XRD methods (in point analysis and mapping mode) have been employed as principal techniques of analysis of these degradation layers due to their sensitivity in discriminating between the valence state of the same element and/or in providing spatially resolved elemental or species-specific information at the micrometer scale [6,36,37].

With the final aim to improve the long-term storage conditions of masterpieces, it becomes relevant to assess the consequences of temperature and humidity (thermal aging) on the photochemical reactivity of light-sensitive pigments in an oil medium.

Similarly to the above-mentioned pigments, also chrome yellows ($PbCr_{1-x}S_xO_4$, with $0 \leq x \leq 0.8$) belong to the category of the light-sensitive compounds. Our previous investigations conducted on photochemically aged oil model paints [38,39,40] and several paint micro-samples taken from paintings by Vincent van Gogh [41,42,43] showed that the degradation process is due to the reduction of the original chromate-anions to Cr(III)-compounds. The photo-reduction is favored when the pigment is present in its orthorhombic and sulfate-rich form ($PbCr_{1-x}S_xO_4$, with $x \geq 0.5$) [39]. Electron energy loss spectroscopy (EELS) investigations allowed us to propose a nano-scale degradation model in which moisture is assumed to play the role in driving the reduction process between the oil binder and the chromate [44]. Moreover, a more recent study has proved that paramagnetic Cr(V)-intermediates are thermally formed through the interaction of the pigment with the oil binder [40], suggesting that a one-electron-transfer may be a part of the reduction mechanism of chromates in an oil painting matrix. These observations have driven the present study where the effect of temperature and humidity on the (photo)reduction process of lead chromate in oil paint has been evaluated to establish *i)* if the darkening of chrome yellows can be caused by thermal aging and *ii)* if the thermal aging affects the photo-induced reduction process.

To this purpose, a multi-method approach based on the combination of diffuse reflectance UV-Vis and attenuated total reflection (ATR)/reflection mode FTIR spectroscopic techniques and metal-

ACCEPTED MANUSCRIPT

speciation methods, namely SR-based μ-XANES/μ-XRF analysis and X-band (*ca.* 9 GHz) electron paramagnetic resonance (EPR) spectroscopy, was used for studying a series of laboratory-prepared $PbCrO_4$, $PbCrO_4{\cdot}PbO$ and $PbCr_{0.2}S_{0.8}O_4$ oil paint models (*i.e.*, with composition similar to that found on a series of paintings by Van Gogh and contemporaries) [45,46], that were first artificially aged with different temperature/relative humidity (RH) conditions in the dark and then exposed to UVA-Vis light.

Diffuse reflectance UV-Vis and ATR/reflection mode FTIR spectroscopies were used to obtain information associated with chromatic changes and to monitor the formation of organo-metal degradation products at the paint surface with aging time. SR-based Cr K-edge μ-XANES/μ-XRF mapping analyses were employed to gain insight into the amount, distribution, and nature of reduced Cr-compounds within the paints with micrometric spatial resolution. EPR spectroscopy was used as a complementary bulk-technique to SR-based X-ray spectromicroscopic methods due to its specificity and sensitivity in detecting paramagnetic Cr(V)-species. These results were compared with those obtained from materials present in a late 19^{th} century historical chrome yellow oil paint tube.

ACCEPTED MANUSCRIPT

2. MATERIALS AND METHODS

2.1. Paint models

2.1.1. Preparation. Paint models were prepared by mixing $PbCrO_4$, $PbCr_{0.2}S_{0.8}O_4$ and $PbCrO_4{\cdot}PbO$ with linseed oil in a 4:1 mass ratio. These mixtures were applied on areas of about 1.5×1.5 cm^2 to a polycarbonate support. The synthesis of monoclinic $PbCrO_4$ (henceforth denoted as S_{1mono}) and of (mainly) orthorhombic $PbCr_{0.2}S_{0.8}O_4$ (S_{3D}), along with a detailed discussion of their chemical and structural properties, is reported in our previous study [45].

The pigment monoclinic $PbCrO_4{\cdot}PbO$ (chrome orange, S_{CO}) was prepared, as described by Xiang *et al.* [47], from a mixture of aqueous solutions of lead(II) acetate and K_2CrO_4 (both 0.2 M) in a 1:1 molar ratio that was kept under magnetic stirring at pH~12. The powder XRD pattern (not shown) was consistent with the expected monoclinic structure of the synthesized pigment, with lattice parameters [a=14.0236(2) Å, b=5.67789(7) Å, c=7.14784(9) Å and β=115.2376(9)°] in line with those reported in the literature for $PbCrO_4{\cdot}PbO$ [47].

2.1.2. Accelerated aging experiments. Once the paint models were touch-dry (after about one month), they were placed in two sealed vessels maintained at different RH conditions: *ca.* 50% using a $Mg(NO_3)_2{\cdot}6H_2O$ (Sigma Aldrich) saturated solution and >95% with distilled water. Both vessels were kept in the dark at 40°C for an overall period of 220 days. Similar aging experiments were also performed on paints made up of pure linseed oil.

At the end of the thermal treatment, paints were subject to UVA-Vis photochemical aging by means of a UV-filtered 175 W Cermax xenon lamp (λ≥300 nm), see ref. [40] for the spectral profile. The measured illuminance and temperature at the sample position were ~1.65×10^5 lux and 40 °C, respectively. Paints were irradiated for 118 hours (total luminous exposure: ~1.95×10^7 lux·h) and at environmental humidity (about 45% RH).

2.2. Late 19th century historical chrome yellow pigment

The pigment was taken from a historical oil paint tube belonging to the Flemish Fauvist Rik Wouters (1882−1913). It is labeled as *Jaune de Chrome* and was produced by Mommen & Cie

ACCEPTED MANUSCRIPT

(Brussels), a company that does not exist anymore and that was a sponsor of Wouters. This material is composed of orthorhombic $PbCr_{0.4}S_{0.6}O_4$ mixed with oil. It was artificially aged with UVA-Vis light for about 800 hours. Further details about the chemical composition, the aging conditions and the photo-chemical reactivity of the pigment are described in our previous studies [38,39,45].

2.3. Analytical methods

2.3.1. UV-Vis. A JASCO V-570 spectrophotometer was used for investigating the unaged paints and those thermally treated before and after UVA-Vis light exposure. Diffuse reflectance spectra were recorded in the 200-850-nm range with a 5 nm spectral bandwidth. The software interfaced with the instrumentation allowed for the conversion of the spectra into CIE L*a*b* chromatic coordinates under standard illuminant D65 and 10° angle observer. Total color changes were calculated according to CIE 1976 formula, $\Delta E^*=(\Delta L^{*2}+\Delta a^{*2}+\Delta b^{*2})^{1/2}$.

2.3.2. FTIR. A portable ALPHA spectrometer (Bruker Optics, Germany/USA) was used for performing ATR and reflection mode measurements of the paint models and of the historical paint before and after aging.

Absorbance spectra were collected by means of a Platinum QuickSnap^{TM} ATR sampling module (A220/D-01) equipped with a diamond crystal plate. Data were recorded in the 4000-375 cm^{-1} range, at a 4 cm^{-1} spectral resolution and with 168 scans.

Pseudo-absorption spectra [Log(1/R); R=reflectance] were obtained using an external reflection module from areas of about 5 mm diameter. Data were acquired in the 6000-375 cm^{-1} range, at a resolution of 4 cm^{-1} and with 186 scans.

Between 3 and 5 spectra were collected from the surface of thermally aged paints after 30, 60, 90, 120, 155, 185 and 220 days. The spectral profiles collected from the paints made up of pure linseed oil did not show significant changes with aging time, thus a selection of them are discussed only in the Supplementary material.

Regarding the photochemically aged samples, analyses of the model paints and of the historical material were performed only at the end of the aging treatment.

ACCEPTED MANUSCRIPT

2.3.3. SR-based μ-XANES/μ-XRF at the Cr K-edge. Thermally aged paints were analyzed before and after light-exposure in the form of thin sections (5-10 μm in thickness) at the X-ray microscope beamline ID21 of the European Synchrotron Radiation Facility (ESRF, Grenoble, FR) [48].

A highly monochromatic primary beam (with $\Delta E/E=10^{-4}$) was obtained with a Si(220) fixed-exit double-crystal monochromator. Kirkpatrick-Baez mirrors were used for focusing the incident beam down to a size of 0.8×0.3 μm² (h×v). Around the Cr K-edge energy range (5.96-6.09 keV), the stability of the beam was within 0.5 μm and 0.3 μm in the vertical and horizontal directions, respectively.

XRF signals were collected in the horizontal plane and at 69° with respect to the incident beam direction using a single energy-dispersive silicon drift detector (Xflash 5100, Bruker). Two-dimensional μ-XRF mapping experiments were performed *via* raster scanning of the samples using the focused X-ray beam and with dwell times of 100 ms/pixel. The PyMca software [49] was used to obtain the elemental distributions. The experimental procedure employed for acquiring and producing the Cr(VI)/Cr(III) chemical state maps is reported elsewhere [38].

μ-XANES spectra in XRF mode were recorded by scanning the primary energy across the Cr K-edge with energy increments of 0.2 eV. A series of one dimensional profiles was collected acquiring a set of μ-XANES spectra along a line perpendicular to the exposed surface of each aged sample.

Since previous EPR investigations established that not only Cr(III)-compounds but also Cr(V)-species are present in the paint samples [40], XANES measurements of a commercially available Cr(V)-reference powder, namely sodium bis(2-hydroxy-2-methylbutyrato)oxochromate(V) [Sigma Aldrich; $NaCrO_5(C_5H_8O)_2$], were carried out by employing an unfocussed X-ray beam (diameter of 200 μm). Because of the sensitivity of Cr(V)-compounds towards reduction under exposure to the X-ray beam [50], preliminary tests were performed to minimize/avoid the damage of the powder.

The ATHENA software [51] was used for the normalization and the linear combination fitting of the spectra against a library of XANES spectra of Cr-reference compounds. This procedure allowed

ACCEPTED MANUSCRIPT

the average relative amount of Cr(VI)-species (expressed as %[Cr(VI)]/[Cr_{total}]) and reduced Cr (*i.e.*, Cr(V)- and Cr(III)-species, denoted below as %[$Cr_{reduced}$]/[Cr_{total}]) as a function of the depth to be determined in a quantitative manner.

2.3.4. EPR. X-band (ν=9.40965 GHz) EPR spectra of S_{3D} paints before and after aging with 95% RH (220 days) were recorded using a Bruker E500 continuous-wave spectrometer equipped with a SHQ cavity and a continuous flow ^{4}He cryostat (ESR900, Oxford Instruments) for variable temperature measurements. For each sample, g-values (g_{sample}) were obtained by the corresponding resonant field (H^{res}) after calibration against a DPPH sample (g_{DPPH}=2.0037), following the relation:

$$g_{sample} = g_{DPPH} \times H^{res}_{DPPH} / H^{res}_{sample}$$

Data of the aged paint were obtained from a portion of the material that was selectively sampled from the surface. Care was taken to ensure to use the same experimental acquisition parameters for the different samples and to avoid saturating conditions.

ACCEPTED MANUSCRIPT

3. RESULTS AND DISCUSSION

3.1. Thermal aging (temperature and humidity) treatment

3.1.1. UV-Vis and FTIR analysis. In Figure 1A-B photographs of the S_{CO}, S_{1mono} and S_{3D} paints and corresponding ΔE* values after the exposure to different RH conditions (at T=40°C) are compared. After aging at 95% RH (Figure 1B: filled bars), the overall color difference, expressed as ΔE* is rather significant for all the paints, with values of about 8, 14 and 18 for S_{CO}, S_{1mono} and S_{3D}, respectively. The color change is also appreciable for the samples exposed to 50% RH (empty bars), ΔE* values being around 5 and 9 for S_{CO} and S_{1mono}, and around 14 for S_{3D}.

A selection of the ATR mode FTIR spectra obtained from the model paints at different aging steps are shown in Figures 2 and 3. The corresponding reflection mode FTIR spectral profiles provide similar information, despite the bands appear distorted with derivative-like/inverted shapes as described in greater detail in the Supplementary material (Figures S1 and S2; *cf.* also Figure S3 for a selection of equivalent data obtained from the aged unpigmented linseed oil paint).

Under aging at 95% RH (Figure 2), the hydrolysis of triglycerides determines the gradual broadening of C=O ester asymmetric stretching mode [ν_a(C=O)] at ~1735 cm^{-1} and the progressive intensity increase of the 1715-1705 cm^{-1} band, ascribable to the ν_a(C=O) mode of free fatty acids [4,5]. With increasing aging time, ν(CH) signals (3100-2800 cm^{-1}) become sharper and shift toward lower wavenumbers. No appreciable changes are visible in the $\nu_a(CrO_4^{2-})$ region (900-800 cm^{-1}).

A broad $\nu_a(COO^-)$ band at 1570-1590 cm^{-1} is visible in the spectra of all samples after treatment for 60 days. This spectral feature resembles that observed in a ZnO oil paint matrix, suggesting the formation of either chemisorbed [52] or amorphous carboxylates [12].

After 120 days, the broad band is replaced by signals at 1512 and 1540 cm^{-1} ascribable to the $\nu_a(COO^-)$ modes of Pb(II)-carboxylates [4,9,19,21,24]. Only the former is visible, as a shoulder, in the spectrum of S_{1mono}. Other spectral features confirm the presence of Pb(II)-soaps: the $\nu_s(COO^-)$ band at around 1416 cm^{-1} and the series of CH bending modes in the 685-740 cm^{-1} range [9,21,24]. For all samples, Pb(II)-carboxylates bands become well-rendered in the spectra recorded after 220

ACCEPTED MANUSCRIPT

days. Whereas the S_{1mono} and S_{3D} spectral profiles are in line with those of Pb(II)-soaps of saturated fatty acids [*e.g.*, Pb(II)-stearate], for the S_{CO} sample the position and intensity of the $\nu_s(COO^-)$ (~1400 cm^{-1}) and $\nu_a(COO^-)$ (~1505 cm^{-1}) bands are ascribable to the additional contribution of Pb(II)-carboxylates of a unsaturated fatty acid [such as Pb(II)-oleate] [21]. Despite the capability of SR-based μ-XRD to detect Pb(II)-carboxylates in painting materials is reported in the literature [15], mapping measurements of this kind carried out on the thermally aged S_{3D} thin section did not show evidence of these compounds, likely due to their amorphous nature (results not shown; experiments performed at DESY-P06 beamline).

In the 1630-1550 cm^{-1} region, additional bands are visible. These might be attributed to the $\nu_a(C=O)$ modes of low molecular weight oxidation compounds of the oil binder (*e.g.*, aldehydes, carboxylic acids), conjugated C=C bonds with the C=O group [53,54], and/or reduced Cr-organo metal compounds [55,56,57].

Regarding the spectra obtained from the samples aged at 50% RH (Figure 3), appreciable changes are visible only after 220 days. For the S_{CO} and S_{3D} materials, the presence of doublet in the 1545–1510 cm^{-1} range along with signals at 1416 cm^{-1} and in the 750-680 cm^{-1} region again indicate the presence of Pb(II)-carboxylates. The identification of these compounds is not straightforward in the spectra of S_{1mono}, in which a broad band at around 1545 cm^{-1} is observable.

The ATR spectrum of the historical $PbCr_{0.4}S_{0.6}O_4$ oil paint, naturally aged for about 100 years in the dark, shows spectral features similar to those of the thermally aged model paints (Figure 4: black line), clearly indicating the possibility of formation of Pb(II)-soaps under ambient (and dark) conditions and within an extended frame time.

From the above, we can conclude that in the thermally aged model paints studied here, the formation of lead(II)-carboxylates is the result of the reaction between the lead chromate-based pigment and the oil binder. In the historical sample, the same hypothesis can be proposed. In this regard, it worth to mention that no additional Pb-based compounds (such as lead carbonate, lead

ACCEPTED MANUSCRIPT

oxide) have been detected [38,45], suggesting that Pb was introduced only through the chromate-based pigment.

Under similar temperature conditions, the process is moisture-dependent and is favored for S_{CO} (monoclinic $PbCrO_4 \cdot PbO$) and S_{3D} (orthorhombic $PbCr_{0.2}S_{0.8}O_4$) rather than S_{1mono} (monoclinic $PbCrO_4$). These results can be explained by considering that the orthorhombic $PbCr_{0.2}S_{0.8}O_4$ solid solution has the highest solubility [39,45] while PbO features the highest reactivity with the oil binder [10,15,19].

Among the factors that might have contributed to the total color change of the aged paint surfaces both the yellowing of the oil [58] and the formation of reduced Cr-compounds need to be considered. The latter is suggested by a reflectance decrease in the 510-765 nm range of the UV-Vis spectra (Figure 5: black lines) [39,40], resembling the one present in the spectral profiles obtained from the equivalent paints that were exposed to UVA-Vis light only (Figure 5: grey lines).

Motivated by such observations, in the next section the Cr-speciation results obtained from the combination of Cr K-edge SR-based μ-XANES and EPR analysis will be discussed with the aim of elucidating the effects of the thermal aging on the reduction reaction of lead chromate-based pigments and on the nature of the corresponding Cr-alteration products.

3.1.2. Cr-speciation investigations. Figure 6 shows the series of Cr K-edge XANES spectra obtained from cross-sectioned S_{1mono} and S_{CO} samples exposed to 95% RH along with the quantitative $[Cr(VI)]/[Cr_{total}]$ and $[Cr_{reduced}]/[Cr_{total}]$ depth profiles acquired from thermally aged S_{3D} thin sections.

One-dimensional series of Cr K-edge XANES spectra collected from S_{1mono} [Figures 6A and S4A (Supplementary material)], S_{CO} (Figure 6B), and S_{3D} [Figure S4B-C (Supplementary material)] *vs.* depth below the exposed surface demonstrate the reduction of the original Cr(VI). In line with previous studies [38,40], this is demonstrated by the shift of the absorption edge toward lower energies and the decrease of the Cr pre-edge peak intensity at 5.993 keV (*cf.* Figure 7 for a selection of the spectra of Cr-reference compounds). These changes are more pronounced in the spectra

ACCEPTED MANUSCRIPT

collected in the upper 2.5 μm of the S_{3D} sample aged at 95% RH [Figure S4C (Supplementary material)]. As Figure 7 illustrates, although in the pre-edge region the position of the peak shifts from 5.9930 keV to 5.9925 keV for the Cr(VI) and Cr(V)-species, respectively and it is split in two bands of very low intensity at 5.9904 and 5.9945 keV for the Cr(III)-compound, the spectra acquired from the aged samples at different depth (Figure 6A-B and Figure S4) do not show appreciable changes in this energy range (*i.e.*, single peak at 5.993 keV).

Three fitting components, such as (a) $PbCr_{0.2}S_{0.8}O_4$, (b) Cr(III) acetate hydroxide [$(CH_3CO_2)_7Cr_3(OH)_2$], and (c) either a Cr(III)-oxide [*i.e.*, $Cr(OH)_3/Cr_2O_3$] or $Cr_2(SO_4)_3{\cdot}H_2O$ or $NaCrO_5(C_5H_8O)_2$ [*i.e.*, a Cr(V)-compound], were necessary to obtain a good description of the XANES spectra recorded along the first 4 μm of S_{3D} aged at 95% RH [see Table S1 (Supplementary material) for details about the fitting results]. Diversely, the spectra of this sample recorded at greater depth and those of the other paints could be properly fitted by using 2 components only [a Cr(VI)-species plus either Cr(III)- or Cr(V)-species; Table S1].

In general, the best result is obtained when Cr(III)-compounds are included as components of the fit model; nevertheless, since Cr(V)-species have been detected in paint of similar composition *via* EPR spectroscopy,[40] their presence cannot be excluded. It is worth to mention that despite the fact that the pre-edge peak area of the Cr(V)-compound is 2-3 times higher than that of the Cr(III)-material (Figure 7), the fitting models give rise to relative amounts of reduced chromium that only differ in numerical values within 8% (in excess) when the Cr(V)-component is considered (Table S1). For these reasons, average values of the fitting results with Cr(III)- and Cr(V)-compounds have been considered in the following discussion to quantify the $[Cr(VI)]/[Cr_{total}]$ and the $[Cr_{reduced}]/[Cr_{total}]$.

Within the first upper micrometer of S_{1mono} and S_{CO} paints, the average amount of reduced Cr is around 10-13% and 17%, respectively (Figure 6A-B; Table S1), while it reaches 32-34% in S_{3D} (Figure 6C: green line/triangles; Figure S4C and Table S1). For S_{1mono} and $S_{3D,}$ the abundance of

ACCEPTED MANUSCRIPT

reduced Cr progressively decreases with increasing depth down to values of about 8% and 20%, respectively.

μ-XANES investigations of the S_{3D} thin section exposed to 50% RH (Figure 6C: green line/circles; Figure S4B and Table S1) revealed that reduced Cr-species are closely localized at the exposed surface and in abundances not higher than 24%. In the analyzed regions just underneath (1.5-9 μm depth), its amount immediately goes down to values between 7 and 10%. For the S_{1mono} paint [Figure S4A (Supplementary material)] the Cr-speciation results are comparable to those obtained from the equivalent paint aged with 95% RH (*cf*. Figure 6A).

On the basis of the above discussed results, the sensitivity of EPR spectroscopy to detect paramagnetic species, such as Cr(V)-compounds, was complementary used to μ-XANES spectroscopy in order to gain insights into the Cr-speciation of the S_{3D} paint aged with 95% RH.

In Figure 8 the low-temperature (5 K) EPR spectra obtained from the S_{3D} paints before (blue line) and after either thermal aging with 95% RH (black line) or UVA-Vis light exposure (grey line) are compared.

In all the spectra two sharp features are clearly visible at g=1.937±0.001 and g=1.980±0.001. While the latter signal was clearly observed even at room temperature and can be readily attributed to Cr(V)-centers [40], the g value of the former is on the low side of the expected range for Cr(V) and might also be suggestive of isolated (*i.e.*, non-interacting) Cr(III)-centers. Finally, a weak sharp signal at g=2.031±0.001 is visible in the unaged sample: since it accounts for only a minor fraction of the paramagnetic intensity of the spectrum and it does not appear to be related to the aging process, we leave it unassigned.

All these sharp signals are superimposed on a broader feature centered at g=2.0, while another additional broad and structured signal centered at g=4.0 is clearly visible. The two latter features are consistent with literature reported EPR spectra of Cr(III)-carboxylate derivatives [56,59] and with spectra of concentrated Cr(III)-species.

ACCEPTED MANUSCRIPT

While an evaluation *via* EPR of the absolute quantities of Cr(III)- and Cr(V)-species would not provide reliable estimates due to the overlap and structuration of the corresponding signals, it is possible to obtain the qualitative variation of the relative abundance of reduced Cr-species in the different samples. This can be done by analyzing the relative intensities of the sharp signal at g=1.980 [Cr(V)-species] and of the broader features at g=2.0 and g=4.0 [Cr(III)-compounds] in the differently aged samples. Thus, the much higher Cr(V):Cr(III) signal ratio in the thermally aged sample compared to both the unaged and the photochemically aged one is clearly evident.

Taken as a whole, the above-mentioned results suggest that the reduction reaction of the original chromate-anions to Cr(III)- and Cr(V)-compounds has occurred under the employed thermal aging conditions and that is favored for S_{3D} rather than for S_{1mono} and S_{CO} paints.

For S_{3D} the amount of reduced chromium became higher with increasing RH levels. The employed thermal aging gave rise to the formation of Cr(V)-species, of which abundance is higher than those revealed in the equivalent paint only exposed to light. In the latter, reduced Cr was found to be mainly present in the trivalent oxidation state.

For S_{1mono} and S_{CO}, the amount of reduced Cr is similar whatever moisture level is used for aging and is comparable also to those obtained from the equivalent paints that were only photochemically aged (see Figure S5 (Supplementary material) and ref. [40] for further details). Among the set of thermally aged paints, this result suggests that the increased ΔE* in the samples exposed to the highest RH condition [see Figure 1B and par. "3.1.1. UV-Vis and FTIR analysis" for the ΔE* values] is mainly due to the (yellow-brownish) oxidation products of the binder and not to reduction of chromium. The same reason may provide an explanation for the highest ΔE* values obtained from the thermally aged paints when compared to the corresponding ones of the equivalent paints only exposed to UVA-Vis light (*cf.* Figure 1B-C, grey bars: $\Delta E^*_{S_{CO}\text{-"UVA-Vis"}} \sim 4$ and $\Delta E^*_{S_{1mono}\text{-"UVA-Vis"}} \sim 8$).

ACCEPTED MANUSCRIPT

The consequences of the thermal conditions on the photo-chemical reactivity of lead chromates are explored in more detail in the following section by discussing the results obtained from the thermally aged model paints and the historical paint after exposure to UVA-Vis light.

3.2. Exposure of thermally aged model paints to UVA-Vis light

Figure 9 shows the ATR mode FTIR spectra of the thermally aged model paints later on exposed to UVA-Vis light. After photochemical aging an extensive loss of structure is observed for some Pb(II)-carboxylate bands, namely $\nu_s(COO^-)$ and bending modes. A broadening is also visible for the $\nu_a(COO^-)$, ν(CH) and ν_a(C=O) modes along with the comparison of new components (*e.g.*, signal at 1780 cm^{-1}) and/or changes of the relative intensities of the bands in the 1650-1550 cm^{-1} range. No appreciable modifications are observable in the chromate absorption region (900-800 cm^{-1}).

A similar trend can be observed in the spectra of the historical $PbCr_{0.4}S_{0.6}O_4$ oil paint (naturally aged for about 100 years) irradiated with UVA-Vis light (Figure 4: grey line), even though the spectrum is different in the 1650-1500 cm^{-1} range: the marker $\nu_a(COO^-)$ signals of Pb(II)-carboxylates are replaced with a broad band centered at 1574 cm^{-1}.

The above-mentioned modifications suggest that the oxidation of the binder has taken place, through the formation of lower molecular weight degradation products (such as aldehydes, carboxylic acids) [53,60].

In Figures 1A,C and 5 the photographs, the ΔE^* and the diffuse reflectance UV-Vis spectra obtained from the thermally aged model paints after UVA-Vis light exposure are compared with those of the equivalent paints that were only photochemically aged.

Light exposure promoted a visible increment of the darkening of all the thermally aged paints, but in a more pronounced manner for the S_{3D} materials (Figure 1A). Consistent with these visual observations, the UV-Vis spectra of the S_{3D} samples show a strong decrease of the reflectance in the 510-765 nm range (Figure 5: red lines).

After light exposure (Figure 1C: red bars), the ΔE^* of the thermally aged S_{CO} and S_{1mono} samples increases for about 1-3 units, reaching values up to ~9 and ~14, respectively. For S_{3D} paints, the

ACCEPTED MANUSCRIPT

color change increases by factor of two, going up to ~34; these values are comparable to the ones obtained for the photochemically aged paint (Figure 1C, grey bar: $\Delta E^*_{S_{3D}\text{-}\text{“UVA-Vis”}}$ ~34).

Whatever RH conditions is used for the aging, the fitting of the XANES spectra obtained from S_{1mono} and S_{CO} paints [Figure 10A-B and Figure S6A (Supplementary material)] shows that light exposure does not promote significant changes of the relative amount of reduced Cr, with values not above 10-13% [see Table S2 (Supplementary material) for details about the fitting results]. This suggests that the observed darkening is mainly due to the degradation of either the organic binder and/or of the corresponding secondary products.

On the other hand, the chemical state maps of Figure 10C show that the irradiation of S_{3D} paints gives rise to the formation of a superficial Cr(III)-rich layer, while Cr(VI)-species are the main constituents of the yellow paint underneath.

According to the fitting results of the XANES spectra [Figure S6B-C and Table S2 (Supplementary material)] and in line with the EPR analysis (*cf.* par. “3.1.2. Cr-speciation investigations”), reduced Cr-species in the trivalent state [*e.g.,* Cr(III)-acetate hydroxide and Cr(III)-oxides] are the most likely to be present within the first 3-4 µm at the paint surface (*i.e.,* where the reduction process is significant). Notably, the quantitative [Cr(VI)]/[Cr_{total}] and [$Cr_{reduced}$]/[Cr_{total}] depth profiles (Figure 10D1,2) highlight that abundances of reduced Cr between 70% and 25% are localized within the upper 7 µm and 9 µm of the material treated with 95% RH and with 50% RH, respectively. In the equivalent paint that was only exposed to UVA-Vis light (Figure 10D3) these alteration species result in amounts between 55% and 25% as a 4-5 µm thick superficial layer. For all samples, the abundance of reduced Cr decreases down to about 20% at greater depth.

In summary, the above-discussed results show that the employed thermal parameters influence the tendency of only the orthorhombic S_{3D} paints towards photo-reduction. After exposure to light of these thermally aged paints, the thickness of the newly formed photo-degradation layer decreases with increasing moisture levels. This might be explained by considering a surface passivation phenomenon that is activated by humidity in the dark [61,62,63]. Since the amount of reduced Cr at

ACCEPTED MANUSCRIPT

the surface increases with increasing moisture level, the superficial alteration layer produced from higher RH condition is assumed to be more efficient in protecting the deeper region of the paint from the interaction with light. Nevertheless, the average abundance of reduced Cr within the upper 3-4 μm of the paint is similar whatever RH conditions were used for aging (*ca.* 65-70%). In this regard, the modification (yellowing-brownishing) of the organic binder may have contributed to filter light in a more significant manner for the sample exposed to higher moisture levels.

ACCEPTED MANUSCRIPT

ACCEPTED MANUSCRIPT

4. CONCLUSIONS

In this paper, a multi-method approach based on the combination of diffuse reflectance UV-Vis, ATR/reflection mode FTIR, SR-based μ-XANES/μ-XRF and EPR spectroscopies was successfully exploited to study the effect of temperature and humidity on the (photo)redox process of lead chromate-based pigments (namely, $PbCrO_4 \cdot PbO$, $PbCrO_4$, $PbCr_{0.2}S_{0.8}O_4$,) in the oil medium. Whereas diffuse reflectance UV-Vis analysis allow us to preliminary determine to which extent the color alteration of the paint surface is due to secondary products arising from the oxidation process of the oil binder and/or to those of the inorganic pigment, ATR and reflection mode FTIR measurements are suitable for the local monitoring of the ongoing reactions between the oil and pigments and for the characterization of the corresponding degradation products from specific spots at the exposed surface.

Regarding the Cr-speciation methods, SR-based X-ray micro-techniques are most useful to extract high-lateral spatial information about the composition and thickness of the micrometric thin upper alteration layer. On the other hand, although EPR does not provide laterally resolved information, it was complementarily employed, considering its highest sensitivity and specificity to detect the formation of long-lived paramagnetic intermediate-species that might be more sensitive toward X-ray beam damage.

After exposure to different relative humidity conditions, FTIR spectroscopy revealed the presence of lead(II)-carboxylates. The process of formation of these compounds increases with increasing moisture levels and is favored for $PbCr_{0.2}S_{0.8}O_4$ (denoted as S_{3D}) and $PbCrO_4 \cdot PbO$ (S_{CO}) rather than $PbCrO_4$ (S_{1mono}). The greater solubility of the orthorhombic $PbCr_{0.2}S_{0.8}O_4$ solid solution with respect to monoclinic phases and the high reactivity of PbO with the oil binder might explain this result. Lead(II)-soaps were also found on a 100 years old naturally aged historical orthorhombic $PbCr_{0.4}S_{0.6}O_4$ oil paint, suggesting the possibility of formation of these compounds under environmental conditions and within an extended frame time.

ACCEPTED MANUSCRIPT

The monoclinic $PbCrO_4$ and $PbCrO_4 \cdot PbO$ paints showed up to 10-17% average amounts of reduced Cr, irrespective of the relative humidity conditions employed. On the contrary, the reduced Cr-abundance in the orthorhombic $PbCr_{0.2}S_{0.8}O_4$ paints gradually increased with an increase of the moisture level ranging from about 20% to 34%. For $PbCr_{0.2}S_{0.8}O_4$, under the employed thermal conditions, the amount of Cr(V)-compounds is significantly higher with respect to that obtained from the analysis of the equivalent material only treated with light, for which reduced-Cr is mainly present in the trivalent oxidation state. This indicates that the environmental conditions to which the pigment is exposed to play a key role towards the formation of different reduced Cr-based compounds.

Within the limits of the employed aging conditions, the thermal and humidity aging increases the photo-reduction tendency only of the light-sensitive orthorhombic $PbCr_{0.2}S_{0.8}O_4$ pigment, while it does not contribute to the activation of photo-redox processes for the more lightfast monoclinic $PbCrO_4$ and $PbCrO_4 \cdot PbO$ compounds.

The integrated approach here proposed in combination with controlled moisture/temperature conditions and photochemical treatments, could be used for assessing the response of other photo-sensitive pigments. Moreover, on the basis of the comparison with the ATR mode FTIR data, the visualization of the diagnostic bands of metal-carboxylates in the reflection mode FTIR spectra (despite their distorted-shapes) opens up the possibility to use this technique as a valuable tool for the non-invasive monitoring of the presence of these degradation products on oil paintings.

ACCEPTED MANUSCRIPT

ACKNOWLEDGMENTS

This research was supported by the Italian project PRIN-(SICH) and by Belgian Science Policy project S2-ART (BELSPO S4DA), the GOA "SOLARPAINT" (Research Fund Antwerp University, Belgium) and FWO (Brussels, Belgium) projects no. G.0C12.13, G.0704.08 and G.01769.09.

ESRF is acknowledged for the beamtime grants received (HG18, HG26 and in-house experiments).

L.S. and L.M. acknowledge the financial support of Ente-CRF and CNR-Short Term Mobility Programme-2013, respectively.

Thanks are expressed to the Royal Academy of Fine Arts of Antwerp and the Royal Museum of Fine Arts of Antwerp (KMSKA) for providing the historical paint sample.

Prof. Dr. Artem Abakumow (EMAT, University of Antwerp) is acknowledged for the XRD measurements of the synthesized powders.

We thank Dr. G. Falkenberg and the members of his team for their assistance in using beamline P06 for the SR-based μ-XRD experiments.

ACCEPTED MANUSCRIPT

ACCEPTED MANUSCRIPT

REFERENCES

[1] R. L. Feller, Accelerated aging: photochemical and thermal aspects, Getty Publications, Los Angeles, 1995.

[2] K. J. van den Berg, A. Burnstock, M. de Keijzer, J. Krueger, T. Learner, A. de Tagle, G. Heydenreich, Issues in contemporary oil paint, Springer International Publishing, 2014.

[3] K. Keune, Binding medium, pigments and metal soaps characterized and localized in paint cross sections, Ph.D. Dissertation, University of Amsterdam, The Netherlands, 2005.

[4] R. Mazzeo, S. Prati, M. Quaranta, E. Joseph, E. Kendix, M. Galeotti, Attenuated total reflection micro FTIR characterisation of pigment–binder interaction in reconstructed paint films, Anal. Bioanal. Chem. 392 (2008) 65-76.

[5] J. Van der Weerd, A. van Loon, J. J. Boon, FTIR studies of the effects of pigments on the aging of oil, Stud. Conserv. 50 (2005) 3-22.

[6] K. Janssens, M. Alfeld, G. Van der Snickt, W. De Nolf, F. Vanmeert, M. Radepont, L. Monico, J. Dik, M. Cotte, G. Falkenberg, C. Miliani, B. G. Brunetti, The use of synchrotron radiation for the characterization of artists' pigments and paintings, Annu. Rev. Anal. Chem. 6 (2013) 399-425.

[7] W. Anaf, S. Trashin, O. Schalm, D. van Dorp, K. Janssens, K. De Wael, Electrochemical photodegradation study of semiconductor pigments: influence of environmental parameters, Anal. Chem. 86 (2014) 9742-9748.

[8] K. Keune, J. J. Boon, Analytical imaging studies of cross-sections of paintings affected by lead soap aggregate formation, Stud. Conserv. 52 (2007) 161-176.

[9] M. J. Plater, B. De Silva, T. Gelbrich, M. B. Hursthouse, C. L. Higgitt, D. R. Saunders, The characterisation of lead fatty acid soaps in ‘protrusions’ in aged traditional oil paint, Polyhedron 22 (2003) 3171-3179.

[10] C. Higgitt, M. Spring, D. Saunders, Pigment-medium interactions in oil paint films containing red lead or lead-tin yellow, National Gallery Technical Bulletin 24 (2003) 75-95.

[11] M. Cotte, E. Checroun, J. Susini, P. Walter, Micro-analytical study of interactions between oil and lead compounds in paintings, Appl. Phys. A: Mater. Sci. Process. 89 (2007) 841-848.

[12] J. J. Hermans, K. Keune, A. van Loon, Piet D. Iedema, An infrared spectroscopic study of the nature of zinc carboxylates in oil paintings, J. Anal. At. Spectrom. 30 (2015) 1600-1608.

[13] J. van der Weerd, M. Geldof, L. van der Loeff, R. M. A. Heeren, J. J. Boon, Zinc soap aggregate formation in ‘Falling leaves (Les Alyscamps)’ by Vincent van Gogh, Kunsttechnol Konserv. 17 (2003) 407-416.

[14] M. Spring, C. Higgitt, D. Saunders, Investigation of pigment-medium interaction processes in oil paint containing degraded smalt, National Gallery Technical Bulletin 26 (2005) 56-70.

ACCEPTED MANUSCRIPT

[15] N. Salvadó, S. Butí, J. Nicholson, H. Emerich, A. Labrador, T. Pradell, Identification of reaction compounds in micrometric layers from gothic paintings using combined SR-XRD and SR-FTIR, Talanta 79 (2009) 419-428.

[16] M. Spring, C. Ricci, D. A. Peggie, S. G. Kazarian, ATR-FTIR imaging for the analysis of organic materials in paint cross sections: case studies on paint samples from the National Gallery, London, Anal. Bioanal. Chem. 392 (2008) 37-45.

[17] K. Keune, J. J. Boon, R. Boitelle, Y. Shimadzu, Degradation of Emerald green in oil paint and its contribution to the rapid change in colour of the Descente des vaches (1834–1835) painted by Théodore Rousseau, Stud. Conserv. 58 (2013) 199-210.

[18] K. Keune, F. Hoogland, J. J. Boon, D. Peggie, C. Higgitt,. Evaluation of the "added value" of SIMS: a mass spectrometric and spectroscopic study of an unusual Naples yellow oil paint reconstruction, Int. J. Mass Spectrom. 284 (2009) 22-34.

[19] M. Cotte, E. Checroun, J. Susini, P. Dumas, P. Tchoreloff, M. Besnard, P. Walter, Kinetics of oil saponification by lead salts in ancient preparations of pharmaceutical lead plasters and painting lead mediums, Talanta 70 (2006) 1136-1142.

[20] G. Osmond, J. J. Boon, L. Puskar, J. Drennan, Metal stearate distributions in modern artists' oil paints: surface and cross-sectional investigation of reference paint films using conventional and synchrotron infrared microspectroscopy, Appl. Spectrosc. 66 (2012) 1136-1144.

[21] L. Robinet, M. C. Corbeil, The characterization of metal soaps, Stud. Conserv. 48 (2003) 23-40.

[22] J. J. Hermans, K. Keune, A. van Loon, R. W. Corkery, P. D. Iedema, The molecular structure of three types of long-chain zinc (II) alkanoates for the study of oil paint degradation, Polyhedron 81 (2014) 335-340.

[23] J. Catalano, A. Murphy, Y. Yao, F. Alkan, N. Zumbulyadis, S. A. Centeno, C. Dybowsky, ^{207}Pb and ^{119}Sn solid-state NMR and relativistic density functional theory studies of the historic pigment lead–tin yellow type I and its reactivity in oil paintings, J. Phys. Chem. A 118 (2014) 7952-7958.

[24] J. Catalano, A. Murphy, Y. Yao, G. P. Yap, N. Zumbulyadis, S. A. Centeno, C. Dybowski, Coordination geometry of lead carboxylates–spectroscopic and crystallographic evidence, Dalton T. 44 (2015) 2340-2347.

[25] M. Radepont, W. de Nolf, K. Janssens, G. Van der Snickt, Y. Coquinot, L. Klaassen, M. Cotte, The use of microscopic X-ray diffraction for the study of HgS and its degradation products

ACCEPTED MANUSCRIPT

corderoite (α-$Hg_3S_2Cl_2$), kenhsuite (γ-$Hg_3S_2Cl_2$) and calomel (Hg_2Cl_2) in historical paintings, J. Anal. Atom. Spectrom. 26 (2011) 959-968.

[26] M. Radepont, Y. Coquinot, K. Janssens, J. J. Ezrati, W. de Nolf, M. Cotte, Thermodynamic and experimental study of the degradation of the red pigment mercury sulfide, J. Anal. Atom. Spectrom. 30 (2015) 599-612.

[27] K. Keune, J. Mass, F. Meirer, C. Pottasch, A. van Loon, A. Hull, J. Church, E. Pouyet, M. Cotte, A. Mehta, Tracking the transformation and transport of arsenic sulfide pigments in paints: synchrotron-based X-ray micro-analyses, J. Anal. Atom. Spectrom. 30 (2015) 813-827.

[28] G. Van der Snickt, J. Dik, M. Cotte, K. Janssens, J. Jaroszewicz, W. De Nolf, J. Groenewegen, L. van der Loeff, Characterization of a degraded cadmium yellow (CdS) pigment in an oil painting by means of synchrotron radiation based X-ray techniques, Anal. Chem.7 (2009) 2600-2610.

[29] G. Van der Snickt, K. Janssens, J. Dik, W. De Nolf, F. Vanmeert, J. Jaroszewicz, M. Cotte, G. Falkenberg, L. van der Loeff, Combined use of synchrotron radiation based micro-X-ray fluorescence, micro-X-ray diffraction, micro-X-ray absorption near-edge, and micro-Fourier Transform infrared spectroscopies for revealing an alternative degradation pathway of the pigment cadmium yellow in a painting by Van Gogh, Anal. Chem. 84 (2012) 10221-10228.

[30] J. L. Mass, R. Opila, B. Buckley, M. Cotte, J. Church, A. Mehta, The photodegradation of cadmium yellow paints in Henri Matisse's Le Bonheur de vivre (1905–1906), Appl. Phys. A: Mater. Sci. Process. 111 (2013) 59-68.

[31] E. Pouyet, M. Cotte, B. Fayard, M. Salomé, F. Meirer, A. Mehta, E. S. Uffelman, A. Hull, F. Vanmeert, J. Kieffer, M. Burghammer, K. Janssens, F. Sette, J. Mass, 2D X-ray and FTIR micro-analysis of the degradation of cadmium yellow pigment in paintings of Henri Matisse, Appl. Phys. A: Mater. Sci. Process. (2015) DOI: 10.1007/s00339-015-9239-4.

[32] L. Samain, F. Grandjean, G. J. Long, P. Martinetto, P. Bordet, J. Sanyova, D. Strivay, Synthesis and fading of eighteenth-century Prussian blue pigments: a combined study by spectroscopic and diffractive techniques using laboratory and synchrotron radiation sources, Synchrotron Radiat. 20 (2013) 460-473.

[33] L. Samain, G. Silversmit, J. Sanyova, B. Vekemans, H. Salomon, B. Gilbert, F. Grandjean, G. J. Long, R. P. Hermann, L. Vincze, D. Strivay, Fading of modern Prussian blue pigments in linseed oil medium, J. Anal. Atom. Spectrom. 26 (2011) 930-941.

[34] L. Zanella, F. Casadio, K. A. Gray, R. Warta, Q. Ma, J. F. Gaillard, The darkening of zinc yellow: XANES speciation of chromium in artist's paints after light and chemical exposures, J. Anal. Atom. Spectrom. 26 (2011) 1090-1097.

ACCEPTED MANUSCRIPT

[35] F. Vanmeert, G. Van der Snickt, K. Janssens, Plumbonacrite identified by X-ray powder diffraction tomography as a missing link during degradation of red lead in a Van Gogh painting, Angew. Chem. Int. Edit. 127 (2015) 3678-3681.

[36] L. Bertrand, L. Robinet, M. Thoury, K. Janssens, S. X. Cohen, S. Schöder, Cultural heritage and archaeology materials studied by synchrotron spectroscopy and imaging, Appl. Phys. A: Mater. Sci. Process 106 (2012) 377-396.

[37] M. Cotte, J. Susini, J. Dik, K. Janssens, Synchrotron-based X-ray absorption spectroscopy for art conservation: looking back and looking forward, Acc. Chem. Res. 43 (2010) 705-714.

[38] L. Monico, G. Van der Snickt, K. Janssens, W. De Nolf, C. Miliani, J. Verbeeck, H. Tian, H. Tan, J. Dik, M. Radepont, M. Cotte, Degradation process of lead chromate in paintings by Vincent van Gogh studied by means of synchrotron X-ray spectromicroscopy and related methods. 1. Artificially aged model samples, Anal. Chem. 83 (2011) 1214-1223.

[39] L. Monico, K. Janssens, C. Miliani, G. Van der Snickt, B. G. Brunetti, M. Cestelli Guidi, M. Radepont, M. Cotte, Degradation process of lead chromate in paintings by Vincent van Gogh studied by means of spectromicroscopic methods. 4. Artificial aging of model samples of co-precipitates of lead chromate and lead sulfate, Anal. Chem. 85 (2013) 860-867.

[40] L. Monico, K. Janssens, M. Cotte, A. Romani, L. Sorace, C. Grazia, B. G. Brunetti, C. Miliani, Synchrotron-based X-ray spectromicroscopy and electron paramagnetic resonance spectroscopy to investigate the redox properties of lead chromate pigments under the effect of visible light, J. Anal. Atom. Spectrom. 30 (2015) 1500-1510.

[41] L. Monico, G. Van der Snickt, K. Janssens, W. De Nolf, C. Miliani, J. Dik, M. Radepont, E. Hendriks, M. Geldof, M. Cotte, degradation process of lead chromate in paintings by Vincent van Gogh studied by means of synchrotron X-ray spectromicroscopy and related methods. 2. Original paint layer samples, Anal. Chem. 83 (2011) 1224-1231.

[42] L. Monico, K. Janssens, F. Vanmeert, M. Cotte, B. G. Brunetti, G. Van der Snickt, M. Leeuwestein, J. Salvant Plisson, M. Menu, C. Miliani, Degradation process of lead chromate in paintings by Vincent van Gogh studied by means of spectromicroscopic methods. Part 5. effects of nonoriginal surface coatings into the nature and distribution of chromium and sulfur species in chrome yellow paints, Anal. Chem. 86 (2014) 10804-10811.

[43] L. Monico, K. Janssens, M. Alfeld, M. Cotte, F. Vanmeert, C. G. Ryan, G. Falkenberg, D. L. Howard, B. G. Brunetti, C. Miliani, Full spectral XANES imaging using the Maia detector array as a new tool for the study of the alteration process of chrome yellow pigments in paintings by Vincent van Gogh, J. Anal. Atom. Spectrom. 30 (2015) 613-626.

ACCEPTED MANUSCRIPT

[44] H. Tan, H. Tian, J. Verbeeck, L. Monico, K. Janssens, G. Van Tendeloo, Nanoscale investigation of the degradation mechanism of a historical chrome yellow paint by quantitative electron energy loss spectroscopy mapping of chromium species, Angew. Chem. Int. Edit. 52 (2013) 11360-11363.

[45] L. Monico, K. Janssens, C. Miliani, B. G. Brunetti, M. Vagnini, F. Vanmeert, G. Falkenberg, A. Abakumov, Y. Lu, H. Tian, J. Verbeeck, M. Radepont, M. Cotte, E. Hendriks, M. Geldof, L. van der Loeff, J. Salvant, M. Menu, Degradation process of lead chromate in paintings by Vincent van Gogh studied by means of spectromicroscopic methods. 3. Synthesis, characterization, and detection of different crystal forms of the chrome yellow pigment, Anal. Chem. 85 (2013) 851-859.

[46] L. Monico, K. Janssens, E. Hendriks, B. G. Brunetti, C. Miliani, Raman study of different crystalline forms of $PbCrO_4$ and $PbCr_{1-x}S_xO_4$ solid solutions for the noninvasive identification of chrome yellows in paintings: a focus on works by Vincent van Gogh, J. Raman Spectrosc. 45 (2014) 1034-1045.

[47] J. H. Xiang, S. H. Yu, Z. Xu, Polymorph and phase discrimination of lead chromate pigments by a facile room temperature precipitation reaction, Cryst. Growth Des. 4 (2004) 1311-1315.

[48] M. Salomé, M. Cotte, R. Baker, R. Barrett, N. Benseny-Cases, G. Berruyer, D. Bugnazet, H. Castillo-Michel, C. Cornu, B. Fayard, E. Gagliardini, R. Hino, J. Morse, E. Papillon, E. Pouyet, C. Rivard, V. A. Solé, J. Susini, G. Veronesi, The ID21 scanning X-ray microscope at ESRF, J. Phys.: Conf. Ser. 425 (2013) 182004.

[49] V. A. Solé, E. Papillon, M. Cotte, P. Walter, J. Susini, A multiplatform code for the analysis of energy-dispersive X-ray fluorescence spectra, Spectrochim. Acta B 62 (2007) 63–68.

[50] A. Levina, R. Codd, G. J. Foran, T. W. Hambley, T. Maschmeyer, A. F. Masters, P. A. Lay, X-ray absorption spectroscopic studies of chromium(V/IV/III)-2-ethyl-2-hydroxybutanoato(2-/1-) complexes, Inorg. Chem. 43 (2004), 1046-1055.

[51] B. Ravel, M. J. Newville, ATHENA, ARTEMIS, HEPHAESTUS: data analysis for X-ray absorption spectroscopy using IFEFFIT, Synchrotron Radiat. 12 (2005) 537–541.

[52] C. Clementi, F. Rosi, A. Romani, R. Vivani, B. G. Brunetti, C. Miliani, Photoluminescence properties of zinc oxide in paints: a study of the effect of self-absorption and passivation, Appl. Spectrosc. 66 (2012) 1233-1241.

[53] M. Lazzari, O. Chiantore, Drying and oxidative degradation of linseed oil, Polym. Degrad. Stabil. 65 (1999) 303-313.

[54] J. Mallégol, J. L. Gardette, J. Lemaire, Long-term behavior of oil-based varnishes and paints I. Spectroscopic analysis of curing drying oils, J. Am. Oil Chem. Soc. 76 (1999) 967-976.

ACCEPTED MANUSCRIPT

[55] M. Bolte, Y. Israeli, A. Rivaton, L. Frezet, R. A. Lessard, Dichromated photosensitive materials: involvement of the polymeric matrix, Proc SPIE-Int. Soc. Opt. Eng. 5290 (2004) 298–305.

[56] A. Vlachos, V. Psycharis, C. P. Raptopoulou, N. Lalioti, Y. Sanakis, G. Diamantopoulos, M. Fardis, M. Karayanni, G. Papavassiliou, A. Terzis, A nearly symmetric trinuclear chromium(III) oxo carboxylate assembly: preparation, molecular and crystal structure, and magnetic properties of $[Cr_3O(O_2CPh)_6(MeOH)_3](NO_3)\cdot 2MeOH$, Inorg. Chim. Acta 357 (2004) 3162-3172.

[57] B. P. Baranwal, T. Fatma, A. Varma, Synthesis, spectral and thermal characterization of nano-sized, oxo-centered, trinuclear carboxylate-bridged chromium (III) complexes of hydroxycarboxylic acids, J. Mol. Struct. 920 (2009) 472-477.

[58] J. Mallégol, J. Lemaire, J. L. Gardette, Yellowing of oil-based paints, Stud. Conserv. 46 (2001) 121-131.

[59] M. K. Nagi, A. Harton, S. Donald, Y. S. Lee, M. Sabat, C. J. O'Connor, J. B. Vincent, An unsymmetric trinuclear chromium(III) oxo carboxylate assembly: structure and characterization of $Cr_3O(O_2CPh)_4(8\text{-hqn})_3\cdot 1.25CH_2Cl_2$, Inorg. Chem. 34 (1995) 3813-3820.

[60] J. Mallégol, J. L. Gardette, J. Lemaire, Long-term behavior of oil-based varnishes and paints. Photo-and thermooxidation of cured linseed oil, J. Am. Oil Chem. Soc. 77 (2000) 257-263.

[61] F. W. Eppensteiner, M. R. Jenkins, Chromate conversion coatings, Met. Finish. 100 (2002) 479-491.

[62] N. Zaki, Trivalent chrome conversion coating for zinc and zinc alloys, Met. Finish. 105 (2007) 425-435.

[63] H. Luo, X. G. Li, C. F. Dong, K. Xiao, X. Q. Cheng, Influence of UV light on passive behavior of the 304 stainless steel in acid solution, J. Phys. Chem. Solids 74 (2013) 691-697.

ACCEPTED MANUSCRIPT

Captions to figures

Figure 1. (A) Photographs of (from top to bottom) S_{CO} (chrome orange: $PbCrO_4 \cdot PbO$), S_{1mono} ($PbCrO_4$) and S_{3D} ($PbCr_{0.2}S_{0.8}O_4$) oil paints and corresponding final ΔE^* after (B) thermal aging [40°C, 95% and 50% relative humidity (RH), 220 days] and (C) a combination of thermal and UVA-Vis light exposure (red bars). The results obtained from the sample UVA-Vis aged only, are also shown for comparison (grey bars) (see Figure 5 for the corresponding UV-Vis spectra).

Figure 2. Selection of the ATR mode FTIR spectra in the 3080-1310 cm^{-1} (left) and 905-650 cm^{-1} (right) range of S_{CO}, S_{3D} and S_{1mono} paints (from top to bottom) before (blue) and during the thermal aging treatment with 95% RH conditions (black) (see Figures S1 and S2 of the Supplementary material for the corresponding reflection mode FTIR spectra).

Figure 3. Selection of the ATR mode FTIR spectra in the 3080-1310 cm^{-1} (left) and 905-650 cm^{-1} (right) range of S_{CO}, S_{3D} and S_{1mono} paints (from top to bottom) before (blue) and during the thermal aging treatment at 50% RH (black) [see Figure S1 (Supplementary material) for the corresponding reflection mode FTIR spectra].

Figure 4. ATR mode FTIR spectra obtained from the historical $PbCr_{0.4}S_{0.6}O_4$ oil paint before (black) and after UVA-Vis light exposure (grey).

Figure 5. Diffuse reflectance UV-Vis spectra of (A) S_{CO}, (B) S_{1mono} and (C) S_{3D} paints before (blue) and after (black) different RH aging treatments and RH combined with UVA-Vis light exposure (red). For comparison change of similar paint underwent only to UVA-Vis light exposure are reported (grey) (see Figure 1 for the corresponding ΔE*).

Figure 6. Result of the linear combination fitting (magenta) of $PbCrO_4$/$PbCrO_4 \cdot PbO$ and either $NaCrO_5(C_5H_8O)_2$ or organo-Cr(III) compounds to the line of XANES spectra (black) obtained from the thermally aged (A) S_{1mono} and (B) S_{CO} paints. In blue, spectra of the reference compounds. (C) Quantitative $[Cr_{reduced}]/[Cr_{total}]$ (green) and $[Cr(VI)]/[Cr_{total}]$ (red) depth profiles obtained as a linear combination fitting of different Cr-reference compounds to the line of XANES spectra recorded from the thermally aged S_{3D} paints: 95% RH (triangles), 50% RH (circles) [see Table S1 and Figure S4 (Supplementary material) for further details about the fitting results].

Figure 7. Cr K pre-edge peak region of the XANES spectra of a selection of different Cr-reference compounds: $PbCrO_4$ (red), $NaCrO_5(C_5H_8O)_2$ (blue) and $Cr(OH)_3$ (green).

ACCEPTED MANUSCRIPT

Figure 8. Low temperature (5 K) X-band (ν=9.40965 GHz) EPR spectra obtained from the S_{3D} paint before (blue) and after different aging treatments: only UVA-Vis light exposure (grey) and 95% RH (black). Leftmost panel shows the full spectral range, while the rightmost one illustrates a magnification of the g=2.0 region.

Figure 9. ATR mode FTIR spectra obtained from the photochemically aged (from top to bottom) S_{CO}, S_{3D} and S_{1mono} paints, previously subject to 220 days of thermal aging: 95% RH (sold line) and 50% RH (circles) (*cf.* Figures 2-3 to see the corresponding spectra obtained before light exposure).

Figure 10. (A-B) Result of the linear combination fitting (magenta) of $PbCrO_4$/$PbCrO_4$·PbO and either $NaCrO_5(C_5H_8O)_2$ or organo-Cr(III) compounds to the line of XANES spectra (black) obtained from the thermally aged (A) S_{1mono} and (B) S_{CO} paints after UVA-Vis light exposure. (C) RG composite Cr(VI)/Cr(III) chemical state maps [step sizes (h×v): 0.8×0.3 μm^2; dwell time: 100 ms/pixel] and (D) corresponding quantitative $[Cr_{reduced}]/[Cr_{total}]$ (green) and $[Cr(VI)]/[Cr_{total}]$ (red) depth profiles, obtained as a linear combination fitting of different Cr-reference compounds to the line of XANES spectra obtained from the thermally aged S_{3D} paints after UVA-Vis light exposure. In (B3) the results acquired from the photochemically aged paint are also report for a comparison [see Table S2, Figure S6 (Supplementary material) and ref. [40] for details about the fitting results].

ACCEPTED MANUSCRIPT

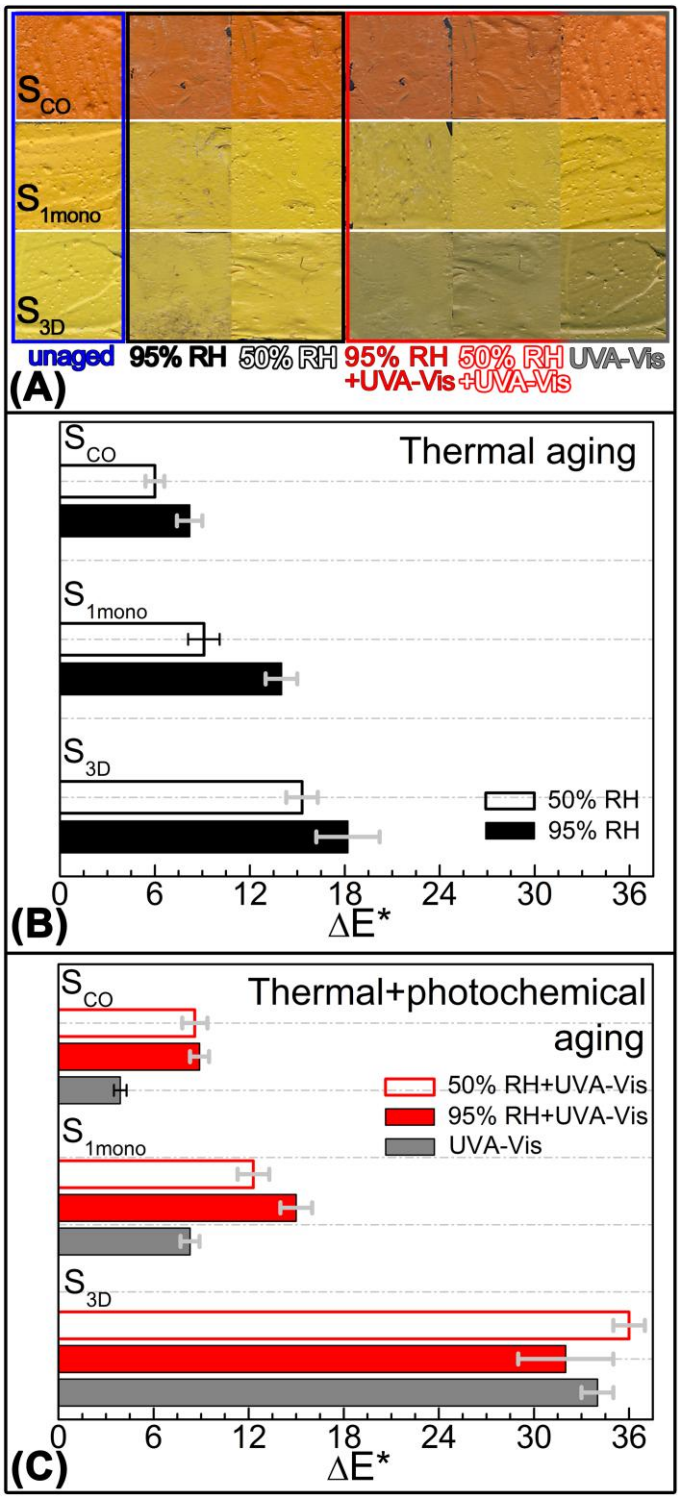

Figure 1

ACCEPTED MANUSCRIPT

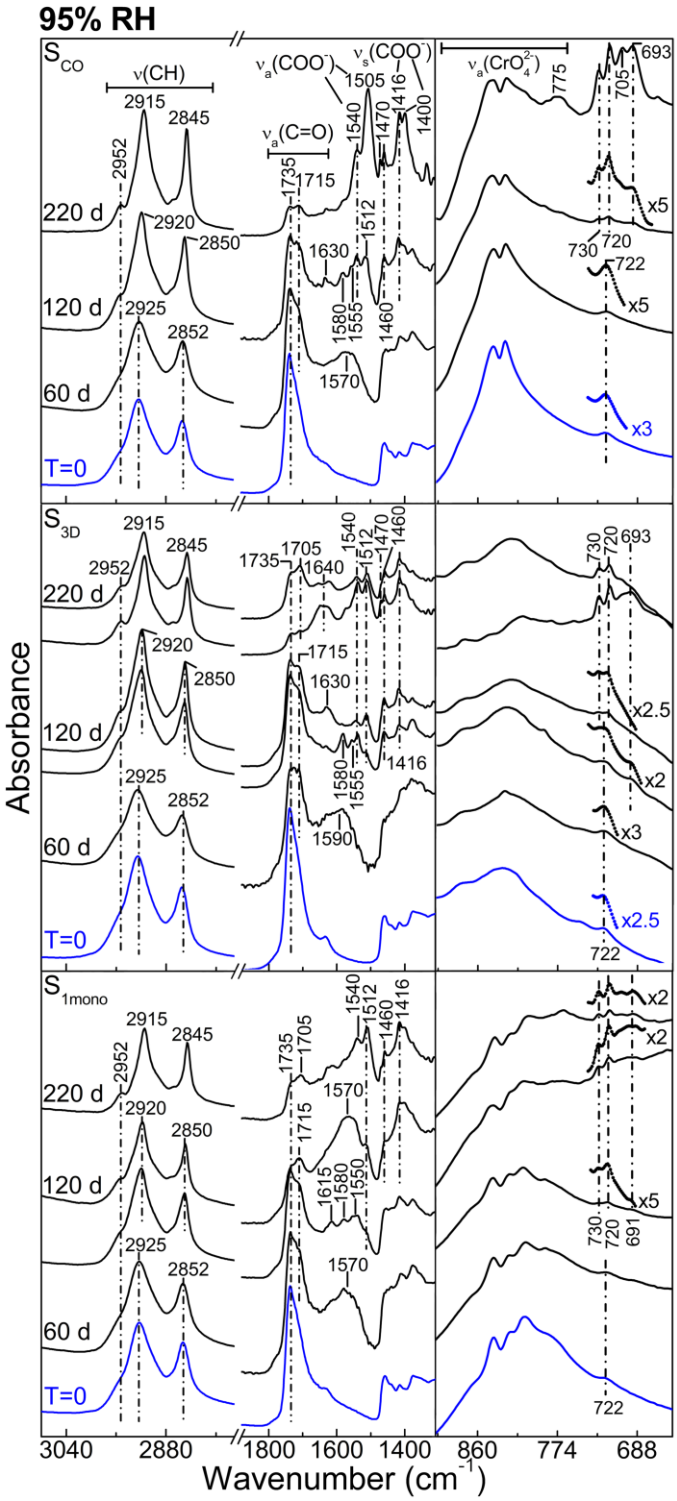

Figure 2

ACCEPTED MANUSCRIPT

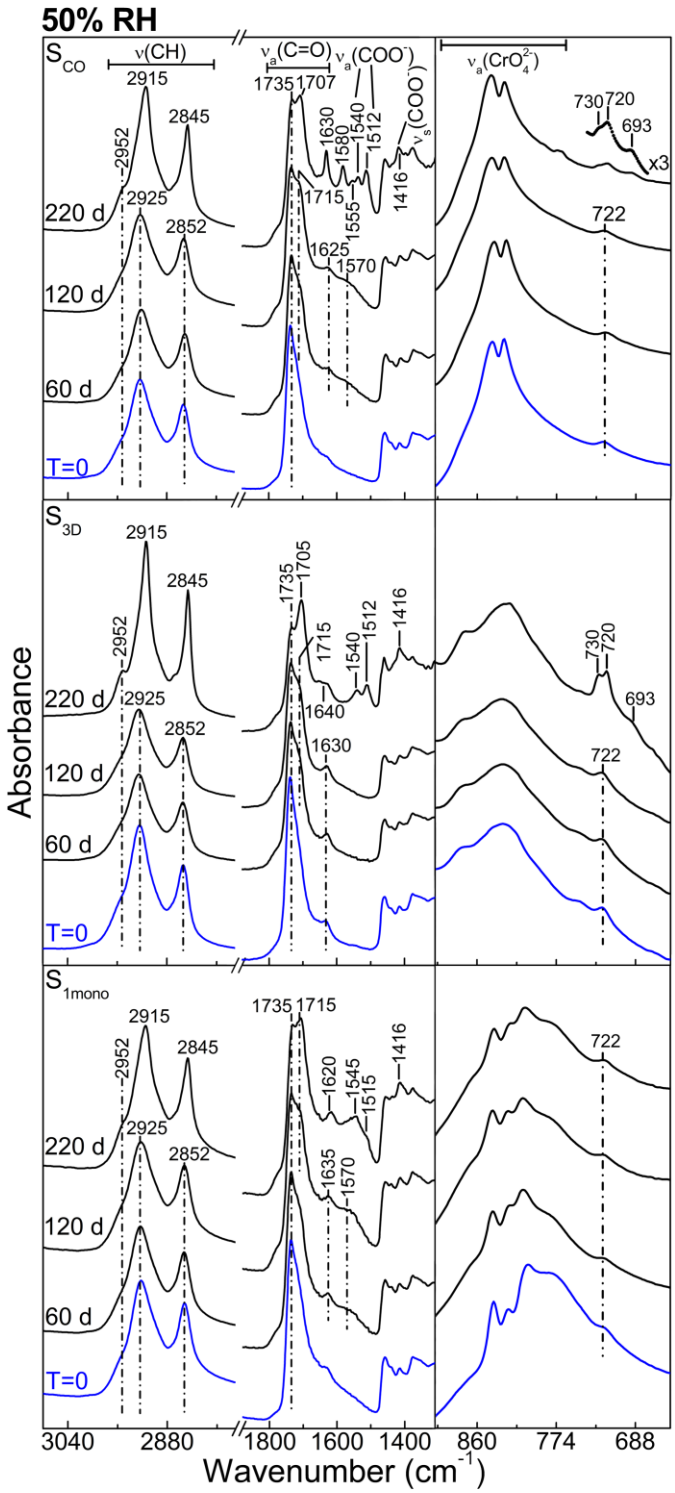

Figure 3

ACCEPTED MANUSCRIPT

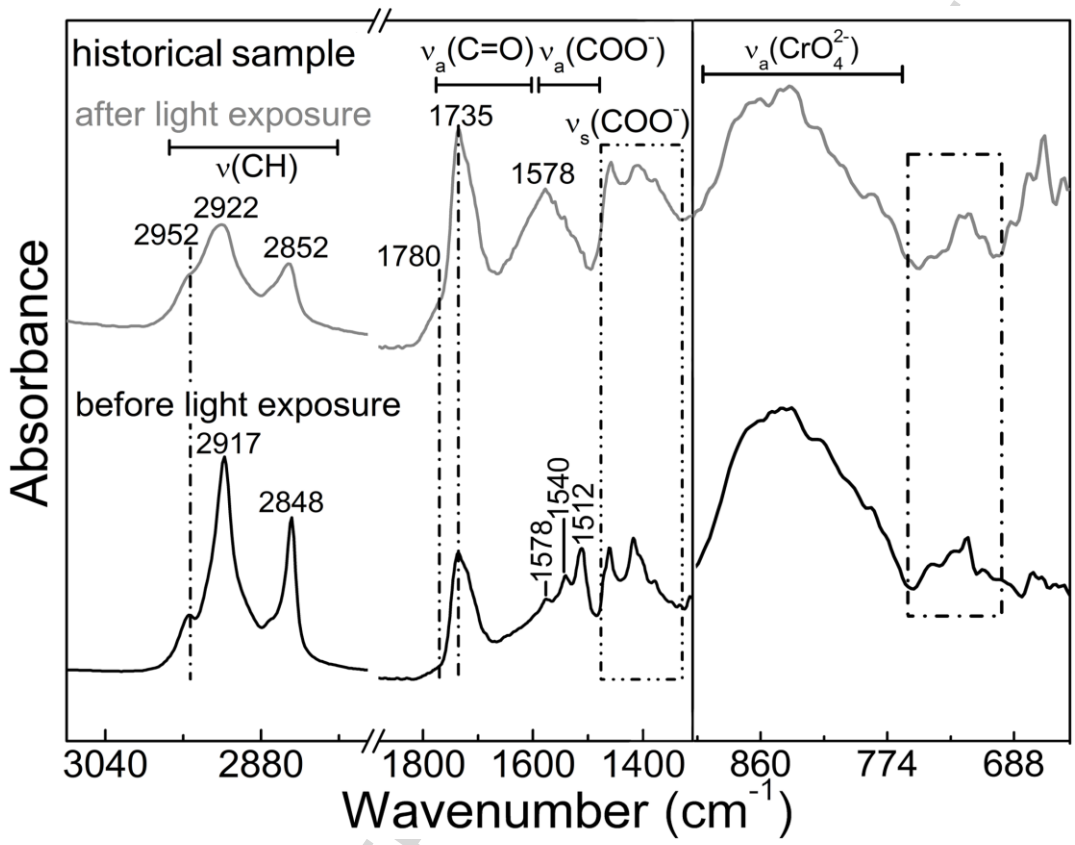

Figure 4

ACCEPTED MANUSCRIPT

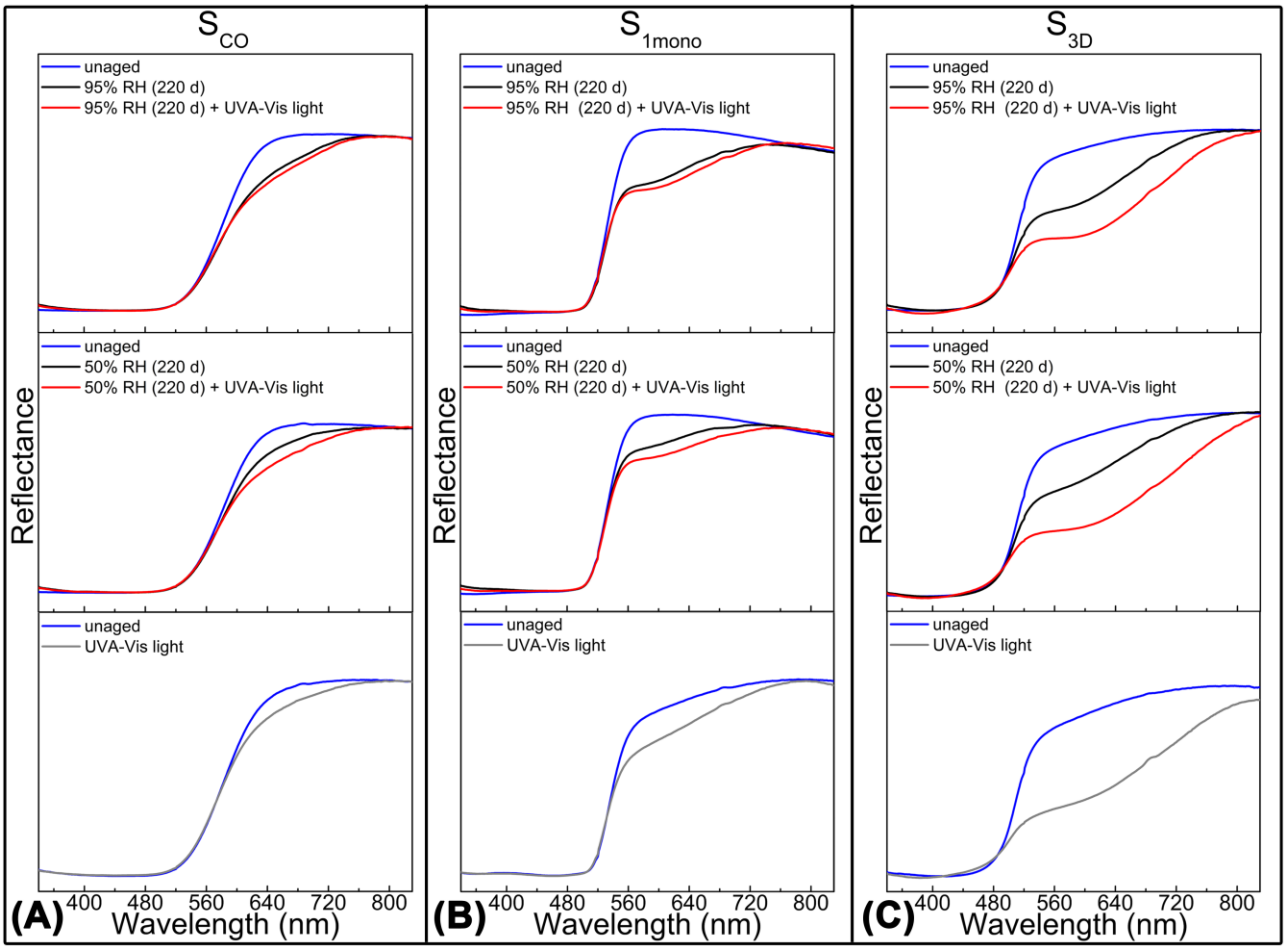

Figure 5

ACCEP

ACCEPTED MANUSCRIPT

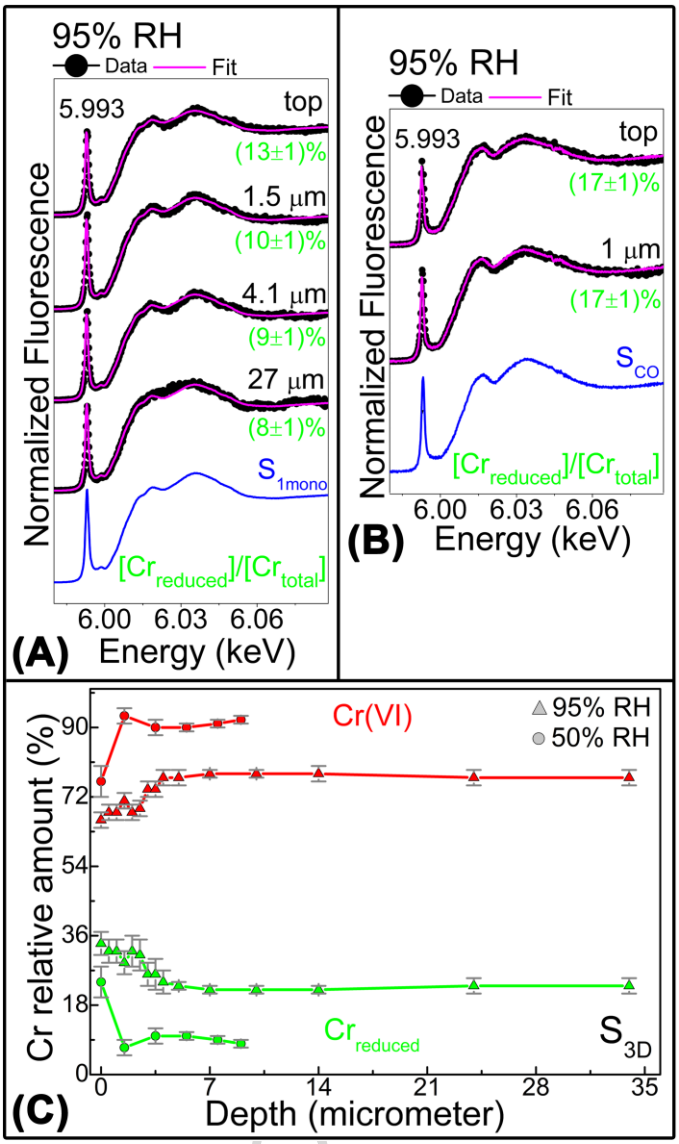

Figure 6

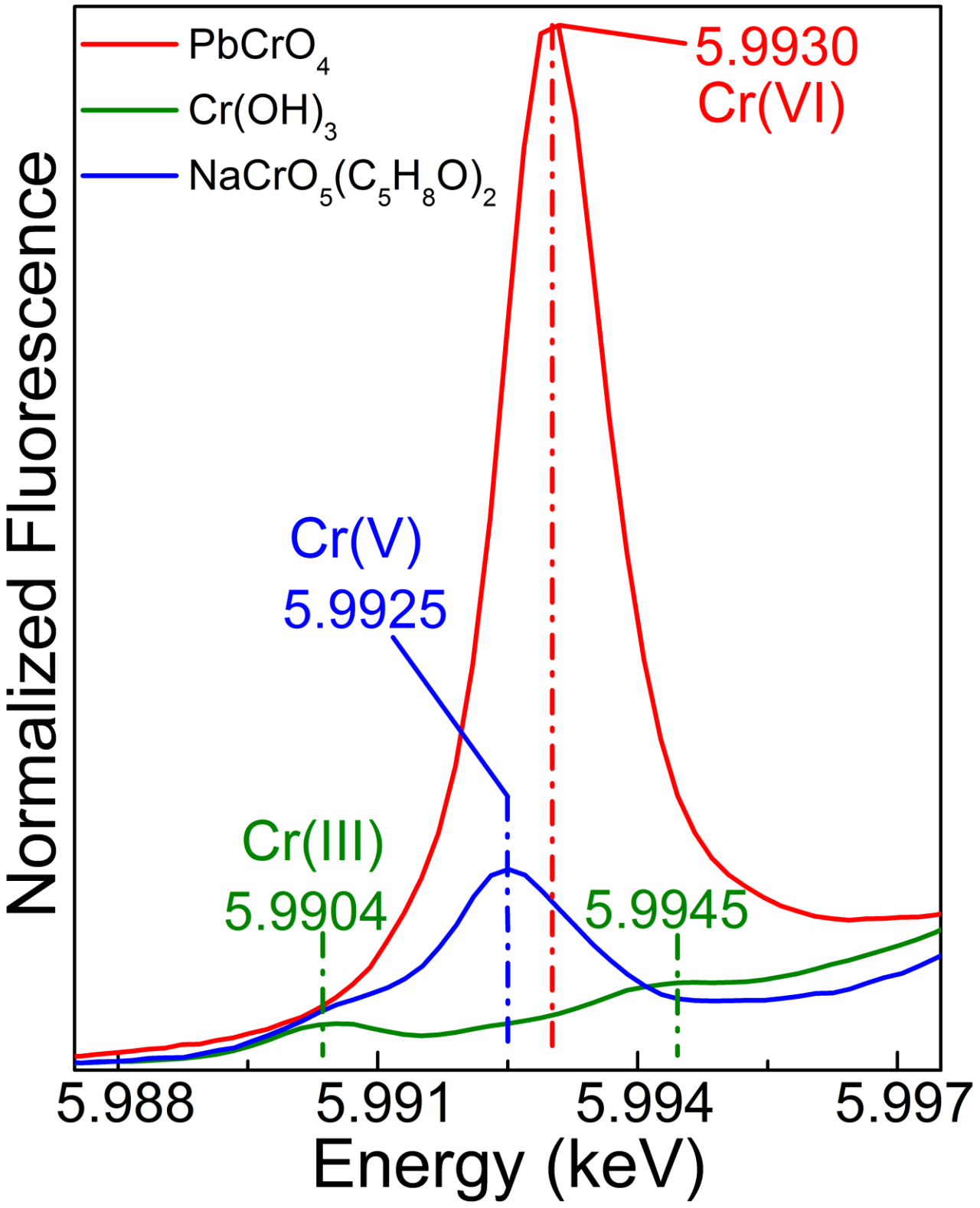
PbCrO4
Cr(OH)3
NaCrO5(C5H8O)2
5.9930
Cr(VI)
Cr(V)
5.9925
Cr(III)
5.9904
5.9945
Normalized Fluorescence
5.988
5.991
5.994
5.997
Energy (keV)

Figure 7

ACCEPTED MANUSCRIPT

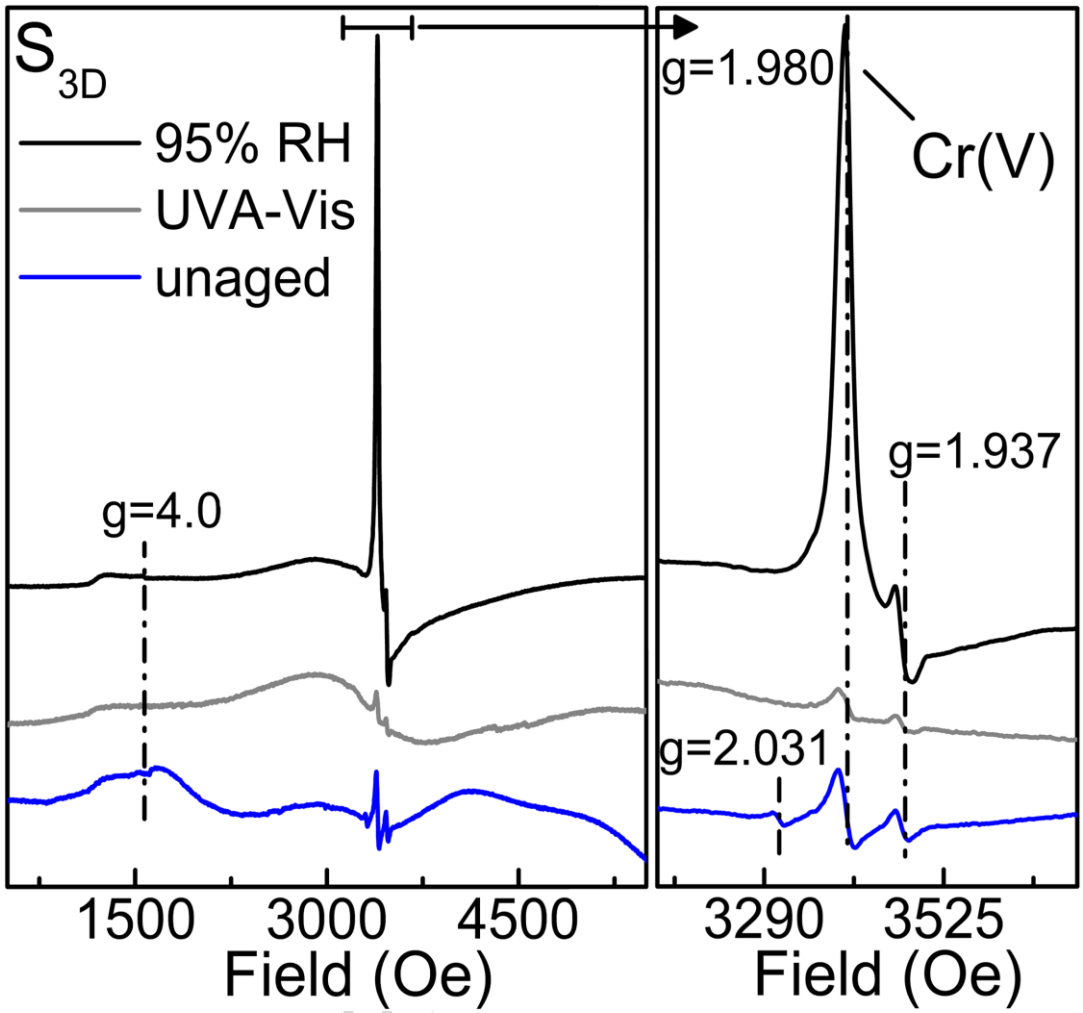

Figure 8

ACCEPTED MANUSCRIPT

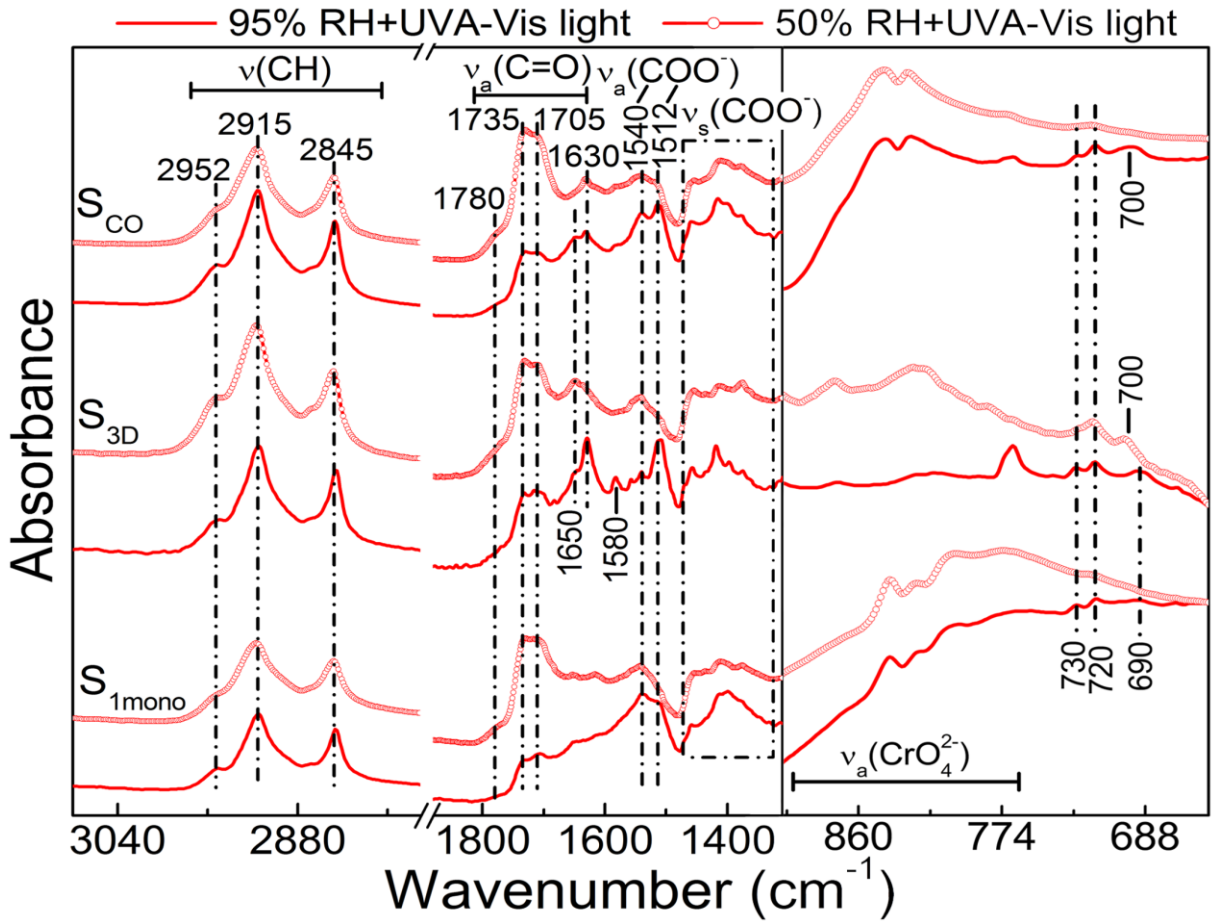

Figure 9

ACCEPTED MANUSCRIPT

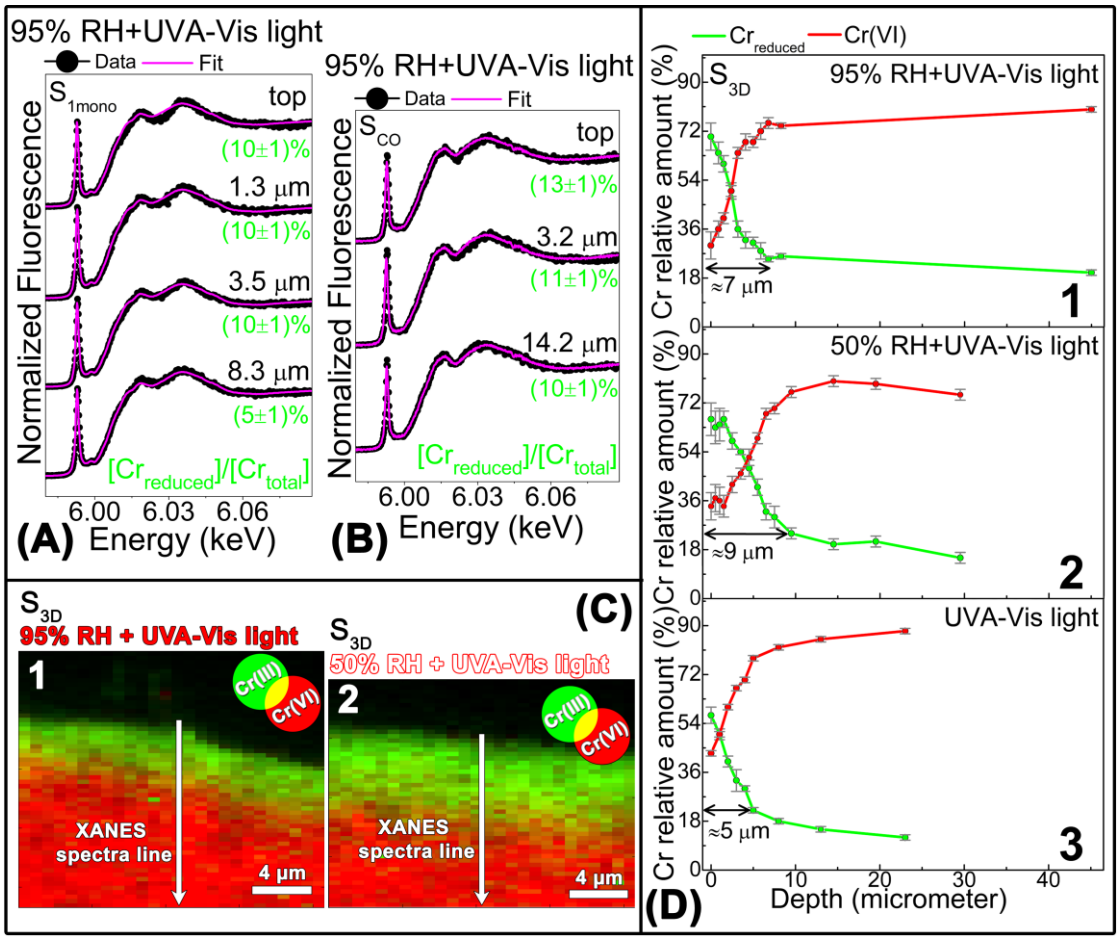

Figure 10

ACCEP

ACCEPTED MANUSCRIPT

HIGHLIGHTS

- The effect of temperature and humidity on the (photo)redox process of different types of lead chromate-based pigments was successfully studied by employing a combination of UV-Vis, FTIR, SR μ-XANES/μ-XRF and EPR spectroscopies.
- Lead(II)-carboxylates, Cr(III)- and Cr(V)-compounds were identified as secondary products of the alteration process and their formation is favored with increasing moisture levels.
- The amount of Cr(V)-species increases when the pigment is treated with humidity, while Cr(III)-alteration products are predominant in the equivalent material only exposed to light.
- The thermal and humidity aging increases the photo-reduction tendency only of the orthorhombic $PbCr_{0.2}S_{0.8}O_4$ pigment, while it does not contribute to the photo-reactivity of the monoclinic $PbCrO_4$ and $PbCrO_4{\cdot}PbO$ compounds.

ACCEPTED MANUSCRIPT